Evolution of feedback-inhibited β/α barrel isoenzymes by gene duplication and a single mutation

Markus Hartmann*, Thomas R. Schneider†, Andrea Pfeil*, Gabriele Heinrich*, William N. Lipscomb‡, and Gerhard H. Braus*§

*Institut für Mikrobiologie and Genetik and †Abteilung für Strukturchemie, Georg August Universität, D-37077 Göttingen, Germany; and ‡Department of Chemistry and Chemical Biology, Harvard University, 12 Oxford Street, Cambridge, MA 02138

Contributed by William N. Lipscomb, December 11, 2002

The β/α barrel is the common protein fold of numerous enzymes and was proposed recently to be the result of gene duplication and fusion of an ancient half-barrel. The initial enzyme of shikimate biosynthesis possesses the additional feature of feedback regulation. The crystal structure and kinetic studies on chimera and mutant proteins of yeast 3-deoxy-D-arabino-heptulosonate-7-phosphate (DAHP) synthase from *Saccharomyces cerevisiae* inhibited by phenylalanine (Aro3p) and DAHP synthase *S. cerevisiae* inhibited by tyrosine (Aro4p) give insight into important regions for regulation in the enzyme: The loop, which is connecting the two half-barrels, and structural elements added to the barrel are prerequisites for regulation and form a cavity on the N-terminal side of the β/α barrel. In the cavity of Aro4p at position 226 is a glycine residue, which is highly conserved in all other tyrosine-regulated DAHP synthases as well. Sequence alignments with phenylalanine-regulated DAHP synthases including Aro3p show a highly conserved serine residue at this position. An exchange of glycine to serine and vice versa leads to a complete change in the regulation pattern. Therefore the evolution of these differently feedback-inhibited isoenzymes required gene duplication and a single mutation within the internal extra element. Numerous additional amino acid substitutions present in the contemporary isoenzymes are irrelevant for regulation and occurred independently.

The β/α barrel is the typical protein fold of a large number of enzymes (1). Evolution of these enzymes is the result of the divergent evolution of a common ancestral barrel, the convergent evolution to a stable three-dimensional structure, or a combination of both. The recent comparison of the β/α barrel structures of two histidine biosynthetic enzymes strongly suggests that these molecules have evolved from an ancestral half-barrel by tandem duplication and fusion (2, 3). For the biosynthesis of the aromatic amino acid tryptophan, most protein structures have been determined and are predominantly folded as eightfold β/α barrels. Many of these enzymes might be the result of gene duplication and gene fusion events and subsequent amino acid substitutions. In addition, distinct protein–protein interactions have been evolved, allowing the formation of oligomeric enzymes (4). The evolution of different enzyme activities requires appropriate changes in the catalytic center of the enzymes, which is localized on the C-terminal face of the central eight-stranded β barrel.

Gene duplication and subsequent alteration can be analyzed in a contemporary cell by comparing isogenes and the corresponding isoenzymes, which are a considerable part of all known enzymes (5). Amino acid sequences of isoenzymes are usually highly similar and allow studies on domains, which have been conserved during the course of evolution.

The initial step of aromatic amino acid biosynthesis is the condensation of erythrose-4-phosphate and phospho*enol*pyruvate (PEP), resulting in 3-deoxy-D-arabino-heptulosonate-7-phosphate (DAHP). The crystal structure of one of the DAHP synthases from *Escherichia coli* consists of an eightfold β/α barrel with several extensions, most notably an N-terminal extension and a two-stranded β-sheet (internal extension) inserted between helix α5 and strand β6 (6). In the budding yeast *Saccharomyces cerevisiae*, the same reaction is catalyzed by two isoenzymes: DAHP synthase from *S. cerevisiae* inhibited by phenylalanine (Aro3p) and DAHP synthase *S. cerevisiae* inhibited by tyrosine (Aro4p) (7). Both proteins consist of 370 amino acids with high sequence homology including 224 identical, 84 similar, and 62 different amino acid residues. The two isoenzymes are differently feedback-regulated by the end products of the pathway, phenylalanine (Aro3p) and tyrosine (Aro4p).

Here, we report the construction and characterization of the regulatory behavior of chimera and mutant proteins of Aro3p (Phe) and Aro4p (Tyr). Together with the crystal structure of Aro4p (Tyr) important modules for regulation are characterized. The exchange of a glycine residue in Aro4p (Tyr) within the regulatory region against a serine residue results in a phenylalanine-regulatable enzyme, which is described.

Materials and Methods

Construction of Chimera Protein. The chimera genes were expressed by using the *MET25* promoter (8) in *S. cerevisiae* strain RH2424 (*MATa, can1-100, GAL, aro3::HIS3, aro4::LEU2, ura3-1*). The chimera fusion genes were constructed within conserved regions to avoid misfolding by the overlapping PCR method. For chimeric gene *3p-4p*, the *ARO3* part was amplified with the oligomers 5′-cgcggatccatgttcattaaaaacgatcacgc-3′ (flanking primer) and 5′-aggccaattctctgtgcagttgg-3′ (overlap primer) and the *ARO4* part with the oligomers 5′-aactgcacagagaattggcct-3′ (overlap primer) and 5′-ggcctcgagttaaaaaaacatctatttcttgttaa-3′ (flanking primer). In a second PCR, both resulting fragments and flanking primers were used to amplify the complete gene. For *3p-(C-4p)*, oligomers 5′-cgcggatccatgttcattaaaaacgatcacgc-3′ and 5′-tctgaaatccttattactgttgccgtg-3′ (*ARO3*) and 5′-ggcaacagtaataaggatttcagaaaccaacca-3′ and 5′-ggcctcgagttaaaaaaacatctatttcttgttaa-3′ (*ARO4*) were used. Oligomers 5′-cgcggatccatgttcattaaaaacgatcacgc-3′, 5′-aggccaattctctgtgcagttgg-3′, 5′-ggtaactccaataaagatttcaagaaccaa-3′, and 5′-ggcctcgagccctcatttacaggctattttt-3′ were used to construct the *ARO3* parts of *3p-4p-(C-3p)*, whereas oligomers 5′-aactgcacagagaattggcct-3′ and 5′-cttgaaatctttattggagttaccgcg-3′ were used to amplify the *ARO4* part. For fusion gene *4p-3p-(C-4p)*, oligomers 5′-cgcggatccatgagtgaatctccaatgttcg-3′, 5′-ggatgctaat-

Abbreviations: PEP, phospho*enol*pyruvate; DAHP, 3-deoxy-D-arabino-heptulosonate-7-phosphate; Aro3p, DAHP synthase from *Saccharomyces cerevisiae* inhibited by phenylalanine; Aro4p, DAHP synthase *S. cerevisiae* inhibited by tyrosine; AroG, DAHP synthase from *Escherichia coli* inhibited by phenylalanine.

Data deposition: The atomic coordinates and structure factors have been deposited in the Protein Data Bank, www.rcsb.org (PDB ID code 1HFB).

§To whom correspondence should be addressed at: Institut für Mikrobiologie und Genetik, Grisebachstrasse 8, D-37077 Göttingen, Germany. E-mail: gbraus@gwdg.de.

tctctgtgcagttgaga-3′, 5′-ggcaacagtaataaggatttcagaaaccaacca-3′, and 5′-ggcctcgagttaaaaaaacatctatttcttgttaa-3′ were used to construct the *ARO4* parts. The *ARO3* part was amplified with the oligomers 5′-caactgcacagagaattagcatccggt-3′ and 5′-tctgaaatcct-tattactgttgccgtg-3′. All plasmid constructs were sequenced completely.

Mutagenesis Experiments with Aro4p. The allelic *ARO4* library was constructed by PCR in the presence of 20 μM Mn^{2+} ions (9). *ARO4* mutant alleles were cloned downstream of the *MET25* promoter, allowing down-regulation to 10% in the presence of 2 mM methionine (8). Tyrosine-resistant mutants were selected on synthetic complete medium lacking aromatic amino acids to screen only for functionally intact DAHP synthases. Mutant colonies were transferred to minimal vitamins medium supplemented with 5 mM tyrosine to reduce DAHP synthase activity and 2 mM methionine to reduce expression of the mutated alleles to screen for alleles encoding tyrosine-resistant Aro4p mutant enzymes. A yeast strain carrying a WT *ARO4* allele as control was not able to grow under these conditions. Mutant plasmids were isolated and retransformed to confirm the phenotype sequences. Deletions and site-directed mutations were introduced by using oligonucleotide mutagenesis and verified by sequencing.

Purification of Enzymes and Determination of Kinetic Data. The mutant DAHP synthases were purified and the kinetic data were determined as described (7, 10). DAHP synthases were detected by SDS/PAGE and enzyme assays (11).

X-Ray Structure Determination. Crystals of DAHP synthase in complex with PEP were grown by the hanging-drop vapor diffusion method at 21°C using a well solution of 14% polyethylene glycol 3000/1 mM DTT buffered at pH 9.0 with 10 mM Tris·HCl (12). The crystals belong to space group P_1 with unit cell constants a = 82.0 Å, b = 93.8 Å, c = 104.5 Å, α = 65.6°, β = 85.6°, and γ = 75.4°. For data collection, a crystal was equilibrated with a solution of 16% polyethylene glycol 3000 buffered at pH 9.0 with 10 mM Tris·HCl and containing 30% glycerol. The glycerol concentration was increased from 5% to 30% in steps of 5%. The data were collected on Beamline X11 at the European Molecular Biology Laboratory at Deutsches Elektronen Synchrotron (Hamburg, Germany) at a wavelength of 0.9076 Å and a temperature of 100 K. The data were integrated, scaled, and merged with DENZO and SCALEPACK (13). Four dimers of DAHP synthase were placed by molecular replacement using the program EPMR (14) with default parameters employing the dimer of chains A and B from *E. coli* DAHP synthase (6). Refinement was performed by using CNS 1.0 (15) with standard command scripts using the maximum-likelihood target function. Eight PEP molecules were included in the model with their stereochemical parameters restrained to standard values as given in the CNS libraries, where available, and with values derived from searches in the Cambridge Structural Data Bank (16) otherwise. All manual rebuilding was performed with XTALVIEW (17). During and after refinement the structure was analyzed by using the programs PROCHECK (18), WHAT IF (19), and LIGPLOT (20). The final model contains 8 molecules of DAHP synthase corresponding to 2,744 protein residues, 8 PEP molecules, and 1,254 water molecules. Only two residues, H282 of molecules D and G, have backbone dihedrals in the disallowed regions of the Ramachandran plot. For both these residues, the electron density is unambiguous. For all eight monomers, no electron density was found for residues M1 to D22. The loop between α8 and β8, which was found to be disordered in the *E. coli* DAHP synthase Pb^{2+} complex, is defined to varying degrees, ranging from the entire loop being ordered in molecule F to the entire loop being disordered in molecule B. The C terminus is defined up to residue N368 in all molecules, with the remaining two residues being visible to varying degrees.

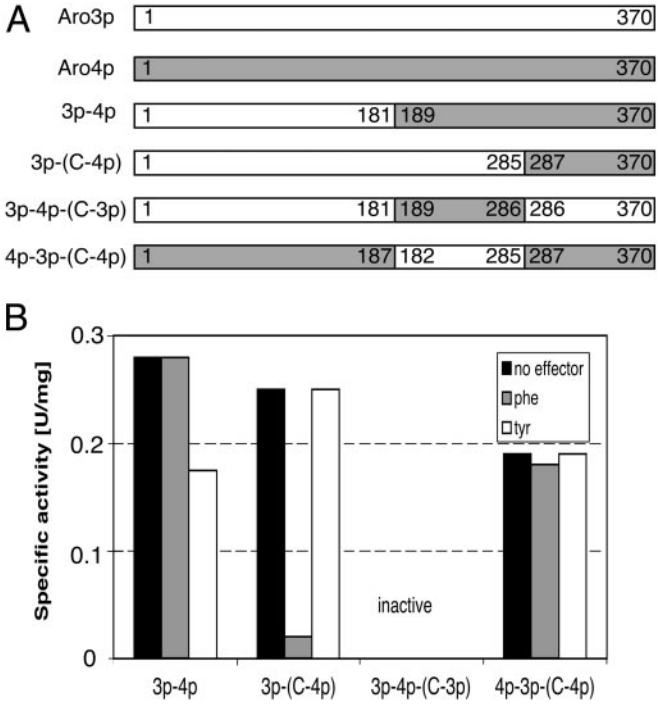

Fig. 1. Regulation of Aro3p/Aro4p chimeric DAHP synthase enzymes of the budding yeast *S. cerevisiae*. (*A*) Schematic structure of various chimeric fusion proteins of Aro3p and Aro4p. Parts of Aro4p and Aro3p are marked in gray and white, respectively, with the indicated amino acid positions as boundaries. (*B*) Specific DAHP synthase activities from yeast crude extracts of the chimera proteins in the presence (gray, 1 mM phenylalanine; white, 1 mM tyrosine) or absence (black) of effector molecules. Enzyme activities are specified in units (1 unit = appearance of 1 μmol product/min). Specific enzyme activities are given as units × ($mg \cdot protein^{-1}$). For comparison, the specific activity of Aro3p without effector is 1.38 units/mg and the specific activity of Aro4p is 1.25 units/mg.

MOLSCRIPT 2.1 (21), RASTER3D (22), and DINO (ref. 23 and www.dino3d.org) were used for the creation of figures as described in the legends.

Results

Aro4p Mutant Enzymes. Chimera proteins were constructed to identify stretches of amino acid residues responsible for a specific distinctive regulatory pattern (Fig. 1). A combination of the N-terminal half of Aro3p (Phe) and the C-terminal half of Aro4p (Tyr) (3p-4p) resulted in an enzyme with significantly reduced enzyme activity (15% in comparison to WT), which is not affected further by phenylalanine and is reduced only slightly by tyrosine (11). Only the combination of the N-terminal and the internal extensions of the same isoenzyme [3p-(C-4p)] resulted in an accurately feedback-inhibited chimera protein. An exchange of the internal part of Aro4p (Tyr) including the two internal β sheets by the corresponding part of Aro3p (Phe) resulted in an unregulated low enzyme activity [4p-3p-(C-4p)], whereas the reverse exchange in Aro3p (Phe) even inactivated the enzyme. These data suggest that the regulation of these isoenzymes involves several parts of the proteins including the N-terminal as well as the internal extensions of the β/α barrel.

To identify single amino acids, which are crucial for regulation, we isolated mutant strains carrying feedback-insensitive Aro4p (Tyr) enzymes (9). The *aro4* alleles with single mutations were identified and localized in the N-terminal extension (D22G, T44I, E49G, and R55G) and in the central part of the enzyme

BIOCHEMISTRY

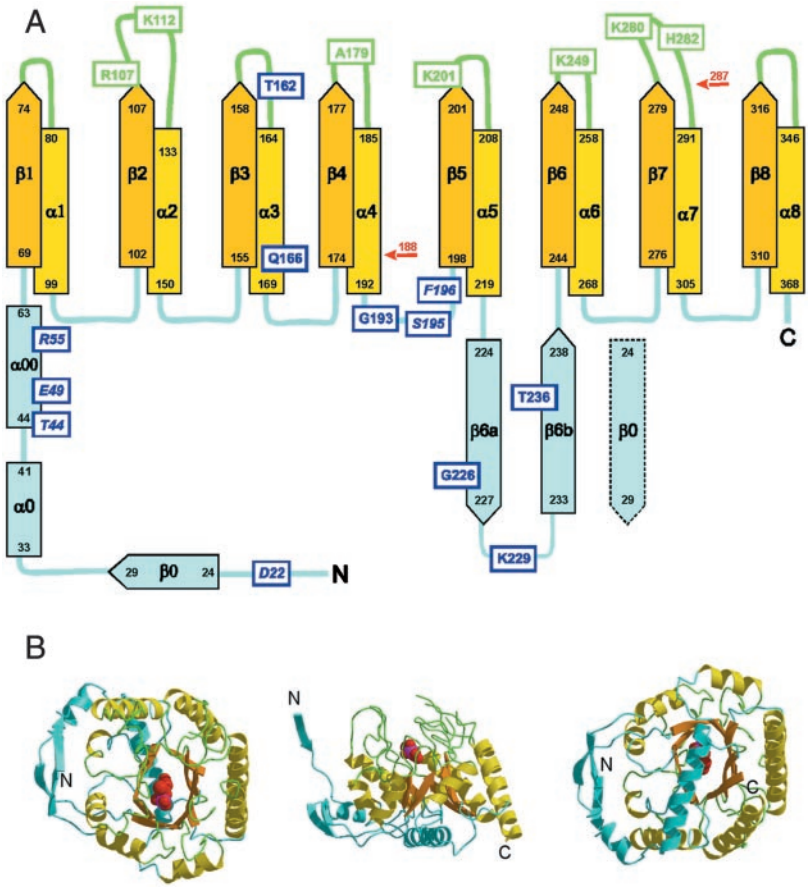

Fig. 2. Aro4p structure of *S. cerevisiae*. (*A*) Topology plot of DAHP synthase from *S. cerevisiae*. The β-strands and α-helices of the central β/α barrel are shown in orange and yellow, respectively. Loops on the N- and C-terminal sides of the barrel are in cyan and green, respectively. The additional structural elements at the N terminus and between helix α5 and β-strand β6 are also shown in cyan. Residues involved in binding of PEP are marked in green. Residues involved in regulation are marked in blue with italic lettering for those identified by random screening and normal lettering for those found by site-directed mutagenesis. Red arrows mark the cutting points in Aro4p for the chimera constructs (Fig. 1*A*). The dotted β0 strand is part of the second monomer of a dimer and interacts with the β6a and β6b. (*B*) The crystal structure of DAHP synthase from *S. cerevisiae* in ribbon presentation. The crystal structures contain a molecule of PEP bound to the active site shown as space-filling models (red and magenta). Secondary structure elements are color-coded as described for *A*. Shown are views from the C-terminal face of the central β barrel (*Left*), side of the barrel (*Center*), and N-terminal face of the barrel (*Right*). The programs MOLSCRIPT 2.1 (21) and RASTER3D (22) were used for the presentation of DAHP synthase.

(S195P and F196S). These latter residues are in fact part of the connector region between the N- and the C-terminal half-barrels (Figs. 2*A* and 3).

Stable deletion of the N-terminal 20 amino acids resulted in an unregulated DAHP synthase with lowered activity in comparison to WT (11%). Both deletion of the N-terminal 32 amino acids and the amino acid residues 220–240 including both internal β strands resulted in completely inactive enzymes. These data suggest that both extensions of the β/α barrel are essential for DAHP synthase activity.

X-Ray Structure. The crystal structure of yeast Aro4p (Tyr) was determined by molecular replacement to 1.9 Å to localize the positions of all amino acid substitutions affecting the tyrosine feedback-inhibition regulatory pattern (Table 1). The x-ray structure of yeast Aro4p (Tyr) (Fig. 2*B*) shows the same fold as the previously determined DAHP synthase from *E. coli* inhibited by phenylalanine [AroG (Phe)] (6). The mean rms deviation for the superposition of 329 equivalent Cα atoms of a molecule of Aro4p (Tyr) onto a molecule of AroG (Phe) is 0.60 Å, indicating an almost identical structure of the polypeptide backbone of these two differently regulated enzymes from different organisms.

Single Amino Acid Exchanges in the Cavity. *ARO4* alleles encoding unregulatable DAHP synthase enzymes possessed amino acid substitutions surrounding a cavity in the x-ray structure. This part of the molecule is defined by α3, α4, the connector between the half-barrels (i.e., loop between β5 and α4), and β6a and β6b (Fig. 3). Specific codons of the *ARO4* ORF were altered to verify whether this cavity represents the regulatory site of the isoenzyme. Single amino acid substitutions of Aro4p (Tyr) in the N-terminal β-sheet β0 (Y28F), the connector region between the half-sites of the regular barrel (G193K, S195A), the internal β-strands β6a (G226A, G226T) and β6b (T236R), and the intervening hairpin loop (K229L) were constructed. In addition, amino acids in the loop preceding helix α3 and α3 itself (T162L, Q166E) located at the bottom of the cavity were changed. The substitutions at positions 162, 193, 195, 226, and 236 had a strong effect on tyrosine inhibition, which was reduced to 20% in the presence of 1 mM tyrosine (WT Aro4p, 98%). Regulation was also diminished by substitutions at position Q166 in α3, K229 in the loop between β6a and β6b and at position T236 in β6b. Substitution at position 28 (β0) had no effect on tyrosine regulation (Fig. 4). All substituted residues at positions 162, 166, 193, 195, 226, 229, and 236 pointed toward an essential role of this cavity for tyrosine regulation of Aro4p (Figs. 3 and 4).

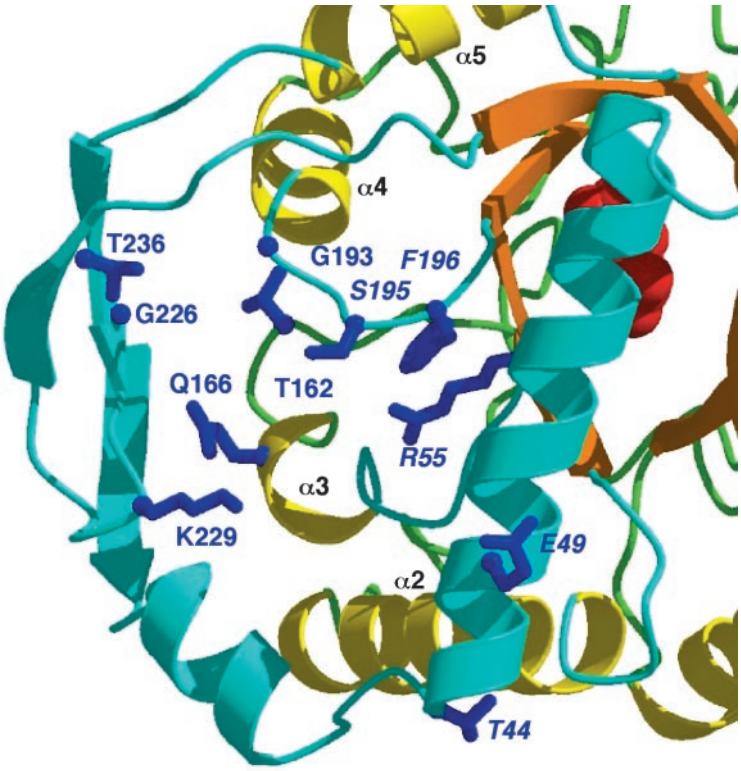

Fig. 3. Magnification of the putative effector-binding cavity of DAHP synthase from *S. cerevisiae*. Secondary structure elements are color-coded as described for Fig. 2. The side chains of residues involved in regulation are shown as blue sticks with italic lettering for those identified by random screening and normal lettering for those found by site-directed mutagenesis. The α-helices α2–α5 are indicated for orientation. The programs MOLSCRIPT 2.1 (21) and RASTER3D (22) were used for the presentation of DAHP synthase.

A comparison of primary sequences of known tyrosine-regulated DAHP synthases and phenylalanine-inhibitable DAHP synthases of various organisms revealed a highly conserved serine residue in all phenylalanine-regulated enzymes at position 219 of yeast Aro3p (Phe) and a highly conserved glycine residue in all tyrosine-inhibitable enzymes at position 226 of yeast Aro4p (Tyr) (Fig. 5*A*). In the three-dimensional structure of yeast Aro4p (Tyr), G226 is located at the bottom of the putative effector-binding cavity (Figs. 3 and 5 *B* and *C*). The corresponding cavity of the phenylalanine-regulated enzyme (AroG) of *E. coli* is reduced significantly when compared with the tyrosine-regulated DAHP synthase of *S. cerevisiae* (Fig. 5 *C* and *D*). This reduction is caused by the side chain of the highly conserved serine in AroG (Phe) pointing into the cavity instead of one single hydrogen contributed by G226 in yeast Aro4p (Tyr).

This difference in the size of the cavity prompted us to ask whether during evolution subsequent to gene duplication a single amino acid exchange would be sufficient to initiate a separation in enzyme regulation toward the distinct effectors phenylalanine or tyrosine. To test this hypothesis, we exchanged the serine at position 219 in Aro3p (Phe) to glycine as well as the glycine at position 226 in Aro4p (Tyr) to serine. The resulting alleles were expressed in yeast, and the mutant enzymes Aro3p-S219G and Aro4p-G226S were purified. The mutant enzymes showed similar activities compared with their corresponding WT enzymes. The k_{cat} values are 8.8 s^{-1} for Aro3p-S219G (Tyr) and 7.9 s^{-1} for Aro4p-G226S (Phe) (Table 2). Surprisingly, the exchange of a single amino acid residue resulted in a completely reversed regulation pattern for both isoenzymes: the formerly phenylalanine-regulated Aro3p enzyme was in its Aro3p-S219G version strongly regulated by tyrosine (K_I = 1.0 μM), and the tyrosine-regulated Aro4p became phenylalanine-inhibitable (K_I = 25 μM). Tyrosine regulation was abolished in the mutant enzyme. Both proteins

Table 1. X-ray data collection, refinement, and model statistics

Resolution range, Å	40.0–1.9
No. of observations	423,490
No. of unique reflections	210,365
R_{sym} (all/high), %	3.7/35.4
Completeness (all/high), %	96.3/89.3
Multiplicity (all/high)	2.9/1.2
$I/\sigma(I)$ (all/high)	13.9/2.2
No. of reflections used in refinement	198,354
No. of reflections in test set	9,891
No. of atoms/$\langle B \rangle$, Å^2	
Protein atoms	20,631/33.4
Ligand atoms	80/31.8
Water sites	1,254/35.7
R_{cryst}, %	20.8
R_{free}, %	26.1
rms deviation from ideal values	
Bond length, Å	0.006
Angles, °	1.3
Dihedral, Å	22.7
Impropers, °	0.79
Ramachandran plot statistics	
Residues in most favored regions, %	90.0
Residues in allowed regions, %	9.9
Residues in disallowed regions, %	0.1

The highest resolution shell contains reflections between 1.97 and 1.90 Å. Statistics were generated with CNS (19) and PROCHECK (20). $R_{sym} = \Sigma|I - \langle I \rangle|/\Sigma|\langle I \rangle|$.

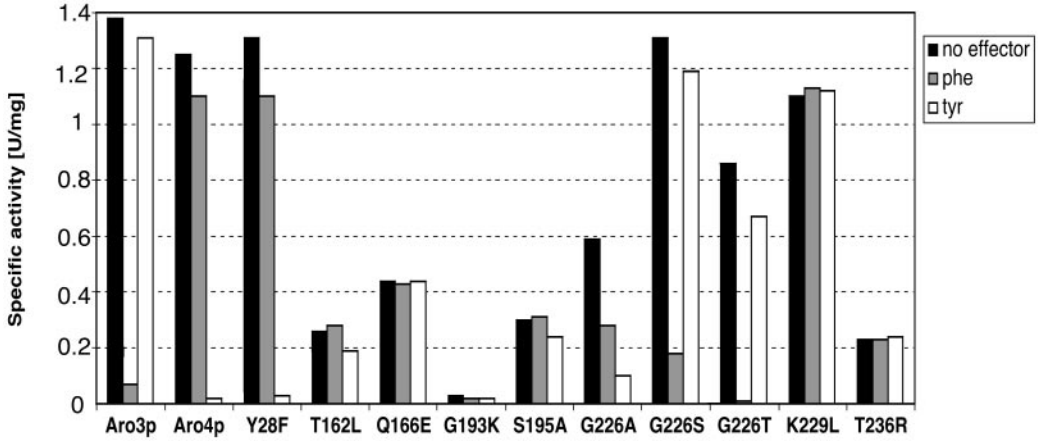

Fig. 4. Specific DAHP synthase activities of Aro4p enzymes carrying various amino acid substitutions introduced by site-directed mutagenesis (Fig. 3). The activities were measured from yeast crude extracts without effector (black) or in the presence of 1 mM phenylalanine (gray) and 1 mM tyrosine (white).

did not change their K_m values toward the substrates PEP and erythrose-4-phosphate.

Discussion

In the evolution of enzymes, there is strong pressure against changes in enzyme structure (5). The structure of an eightfold β/α barrel, first described for the enzyme triose phosphate isomerase (24), is the most common fold for enzymes and is particularly well suited for the evolution of new functions; modifications of the loops between the α-helices and β-strands alter the properties of binding and catalysis without affecting the basic structure of the enzyme (25). The DAHP synthase isoenzymes of yeast as well as *E. coli* represent such extended β/α barrels with the catalytic site on the C-terminal face, as it is in all β/α barrels. In these enzymes, extensions are used to construct a cavity on the N-terminal side of the barrel that possibly facilitates binding of effector molecules.

Distinct α-helices and β-strands had to be added to the β/α barrel to build a cavity required for effector binding and feedback inhibition of the enzymes (Fig. 2*A*). The extra β-sheets

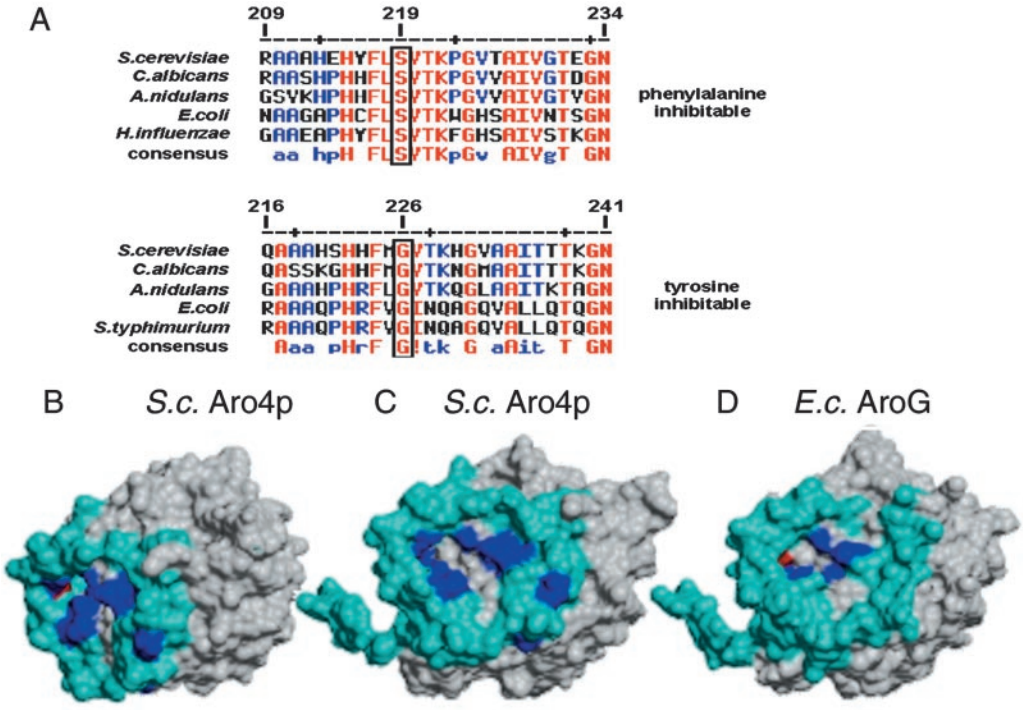

Fig. 5. Comparison of the putative effector-binding cavity of the tyrosine- and phenylalanine-regulated DAHP synthases. (*A*) Amino acid sequence alignment of a part of the putative regulation cavity of the tyrosine- and phenylalanine-regulated DAHP synthases of several organisms. *C. albicans*, *Candida albicans*; *A. nidulans*, *Aspergillus nidulans*; *H. influenzae*, *Haemophilus influenzae*; *S. typhimurium*, *Salmonella typhimurium*. (*B–D*) Accessible surface plots of the tyrosine-regulated DAHP synthase Aro4p from *S. cerevisiae* (*S.c.*, *B* and *C*) and the phenylalanine-inhibited DAHP synthase AroG from *E. coli* (*E.c.*, *D*). Surface elements closer than 3 Å to atoms belonging to the N-terminal extension or the inserted β sheet are shown in cyan. Residues identified as playing a role in regulation (blue) and for the specificity-related residue (red, G226 in Aro4p and S211 in AroG) are indicated. (*B*) The orientation is the same as described for Fig. 2*B*. (*C* and *D*) The view is rotated by 40° around the vertical and 30° around the horizontal axis with respect to Fig. 2*B*. The figure was created with DINO (ref. 23 and www.dino3d.org).

Table 2. Kinetic parameters of the DAHP synthase mutants Aro3p-S219G and Aro4p-G226S from *S. cerevisiae*

	Mutants		WT enzymes	
	Aro3p-S219G	Aro4p-G226S	Aro3p (10)	Aro4p (7)
K_m (PEP), μM	27	122	18	125
K_m (E4P), μM	136	349	130	500
K_i, μM	1	25	10	0.9
k_{cat}, s^{-1}	8.8	7.9	7.0	6.0

The K_i values refer to the specific inhibitor phenylalanine for Aro3p and Aro4p-G226S and tyrosine for Aro4p and Aro3p-S219G.

6a and 6b are absent in a normal β/α barrel fold and had to be inserted into the primary sequence to develop the central regulatory part (amino acids 220–243) within the β/α barrel, which forms the top of the cavity in the three-dimensional structure. In addition, the connector region between the two half-sites is involved in regulation.

The N terminus with its β0 domain is another important module that had to be added to the regular β/α barrel to evolve a regulatory domain. Oligomerization is an important prerequisite for regulation as well, because there is interaction of the β0-sheet of the N terminus with the other monomer. The relevant cavity required for regulation that is located at the top of the enzyme is defined by α3, α4 as regular β/α barrel domains, the half-barrel connector region, and the extra domains β6a and β6b. These parts belong to one monomer and interact with the N-terminal β0 of the neighbor monomer. The N-terminal region, found to be unstructured in both crystals of the *E. coli* and the yeast enzyme, was shown to become structured after the binding of an effector molecule and forming a lid supporting the coordination of the effector (26). Amino acid residue exchanges within this cavity of the tyrosine-regulated isoenzyme resulting in mutant enzymes insensitive toward the effector might prevent this structured conformation, e.g., by the inability of binding tyrosine.

The overall structures derived from the crystal of the eukaryotic tyrosine-regulated DAHP synthase and the prokaryotic phenylalanine-regulated DAHP synthase are nearly identical. The same cavity but with reduced size exists in the phenylalanine-regulated isoenzyme of *E. coli*. The two differently regulated DAHP synthase isoenzymes of *S. cerevisiae* show 62 different amino acids. The evolution of two differently regulated DAHP synthases, however, required only a single amino acid substitution. The highly conserved and small glycine (tyrosine-regulated DAHP synthases) in the central β6a domain increases the space of the cavity. In contrast, the conserved serine (phenylalanine-regulated DAHP synthases) decreases the cavity space. The exchange of this particular amino acid between the differently regulated isoenzymes formed mutant enzymes, which show a completely exchanged regulatory behavior. Aro3p with the S219G exchange was Aro4p-like tyrosine-regulated, and Aro4p with G226S was Aro3p-like phenylalanine-regulated. Therefore, it was possible by *in vitro* evolution to switch the specific regulative behavior of each DAHP synthase isoenzyme from *S. cerevisiae* by keeping 61-aa constant differences and exchanging only the appropriate single amino acid. In contrast to this finding, the amino acid exchange from glycine to alanine at position 226 in the tyrosine-regulated Aro4p does not lead to a change in the inhibitory behavior. This is maybe due to the fact that alanine is not a hydrophobic amino acid and is not that voluminous, as serine is.

In summary, our data suggest that the addition of an N-terminal and central regulatory domain to the primary sequence of the barrel and the development of an additional binding site were necessary extensions for regulation. A single amino acid substitution in the central region of Aro4p, which is not present in a regular β/α barrel, was sufficient to produce a first Aro3p precursor. This residue is located at the cavity required for DAHP synthase regulation. The additional 61 different amino acid residues that can be found in both isoenzymes in our days are irrelevant for regulation.

This work was supported by grants from the Deutsche Forschungsgemeinschaft, the Volkswagen-Stiftung, and the Fonds der Chemischen Industrie (to G.H.B.). Support from National Institutes of Health Grant GM06920 (to W.N.L.) is also acknowledged.

1. Farber, G. K. & Petsko, G. A. (1990) *Trends Biochem. Sci* **15,** 228–234.
2. Lang, D., Thoma, R., Henn-Sax, M., Sterner, R. & Wilmanns, M. (2000) *Science* **289,** 1546–1550.
3. Höcker, B., Beismann-Driemeyer, S., Hettwer, S., Lustig, A. & Sterner, R. (2001) *Nat. Struct. Biol.* **8,** 32–36.
4. Dandekar, T., Snel, B., Huynen, M. & Bork, P. (1998) *Trends Biochem. Sci.* **23,** 324–328.
5. Rider, C. C. & Taylor, C. B. (1980) *Isoenzymes* (Chapman & Hall, New York).
6. Shumilin, I. A., Kretsinger, R. H. & Bauerle, R. H. (1999) *Struct. Fold. Des.* **7,** 865–875.
7. Schnappauf, G., Hartmann, M., Künzler, M. & Braus, G. H. (1998) *Arch. Microbiol.* **169,** 517–524.
8. Mumberg, D., Müller, R. & Funk, M. (1994) *Nucleic Acids Res.* **22,** 5767–5768.
9. Leung, D. W., Chen, E. & Goeddel, D. V. (1989) *Technique (Montreal)* **1,** 11–15.
10. Paravicini, G., Schmidheini, T. & Braus, G. (1989) *Eur. J. Biochem.* **186,** 361–366.
11. Takahashi, M. & Chan, W. W. C. (1971) *Can. J. Biochem.* **49,** 1015–1025.
12. Schneider, T. R., Hartmann, M. & Braus, G. H. (1999) *Acta Crystallogr. D* **55,** 1586–1588.
13. Otwinowski, Z. & Minor, W. (1996) *Methods Enzymol.* **276,** 307–325.
14. Kissinger, C. R., Gehlhaar, D. K. & Fogel, D. B. (1999) *Acta Crystallogr. D* **55,** 484–491.
15. Brunger, A. T., Adams, P. D., Clore, G. M., DeLano, W. L., Gros, P., Grosse-Kunstleve, R. W., Jiang, J. S., Kuszewski, J., Nilges, M., Pannu, N. S., *et al.* (1998) *Acta Crystallogr. D* **54,** 905–921.
16. Allen, F. H. & Kennard, O. (1993) *Chem. Des. Autom. News* **8,** 31–37.
17. McRee, D. E. (1999) *J. Struct. Biol.* **125,** 156–165.
18. Laskowski, R. A., MacArthur, M. W., Moss, D. S. & Thornton, J. M. (1993) *J. Appl. Crystallogr.* **25,** 283–291.
19. Vriend, G. (1990) *J. Mol. Graphics* **8,** 52–56.
20. Wallace, A. C., Laskowski, R. A. & Thornton, J. M. (1995) *Protein Eng.* **8,** 127–134.
21. Kraulis, P. J. (1991) *J. Appl. Crystallogr.* **24,** 946–950.
22. Merritt, E. A. & Murphy, M. E. P. (1994) *Acta Crystallogr. D* **50,** 869–873.
23. Philippsen, A. (2001) DINO (Div. of Struct. Biol., Biozentrum, Univ. of Basel, Basel), Version 0.8.4.
24. Phillips, D. C., Sternberg, M. J., Thornton, J. M. & Wilson, I. A. (1978) *J. Mol. Biol.* **119,** 329–351.
25. Lindqvist, Y. & Brändén, C. I. (1985) *Proc. Natl. Acad. Sci. USA* **82,** 6855–6859.
26. Shumilin, I. A., Zhao, C., Bauerle, R. & Kretsinger, R. H. (2002) *J. Mol. Biol.* **320,** 1147–1156.